NIH Public Access
Author Manuscript
Nanoscale. Author manuscript; available in PMC 2011 April 19.

Published in final edited form as:
Nanoscale. 2011 April 6; 3(4): 1724–1730. doi:10.1039/c0nr00932f.

Gold Nanocages Covered with Thermally-responsive Polymers for Controlled Release by High-intensity Focused Ultrasound**

Weiyang Li[†,a], **Xin Cai**[†,a], **Chulhong Kim**[†,a,b], **Guorong Sun**[a], **Yu Zhang**[a], **Rui Deng**[a], **Miaoxin Yang**[a], **Jingyi Chen**[a], **Samuel Achilefu**[c], **Lihong V. Wang**[*,a], and **Younan Xia**[*,a]

[a]Department of Biomedical Engineering, Washington University, St. Louis, Missouri 63130

[c]Department of Radiology, Washington University School of Medicine, St. Louis, MO 63110

Abstract

This paper describes the use of Au nanocages covered with smart, thermally-responsive polymers for controlled release with high-intensity focused ultrasound (HIFU). HIFU is a highly precise medical procedure that uses focused ultrasound to heat and destroy pathogenic tissue rapidly and locally in a non-invasive or minimally invasive manner. The released dosage could be remotely controlled by manipulating the power of HIFU and/or the duration of exposure. We demonstrated localized release within the focal volume of HIFU by using gelatin phantom samples containing dye-loaded Au nanocages. By placing chicken breast tissues on top of the phantoms, we further demonstrated the feasibility of this system for controlled release at depths up to 30 mm. Because it can penetrate more deeply into soft tissues than near-infrared light, HIFU is a potentially more effective external stimulus for rapid, on-demand drug release.

Keywords

Gold; nanocages; high-intensity focused ultrasound; controlled release

Introduction

Gold (Au) nanostructures have received considerable attention in biomedical research owing to their spectacular optical properties, bio-inertness, and low cytotoxicity.[1] Among various Au nanostructures, nanocages characterized by hollow interiors and thin, porous walls are of paticular interest for biomedical applications, with notable examples including imaging, cancer targeting, and photothermal treatment.[2] The unique porous structure of nanocages also enables additional applications, especially in drug delivery, by delivering a chemical species pre-stored in the hollow interior of a nanocage. The localized surface plason resonance (LSPR) peak of nanocages can be precisely tuned to the near-infrared (NIR) region from 700 to 900 nm, where the attenuation of light by blood and water is relatively low. Our previous work has demonstrated the use of Au nanocages covered with smart

**Electronic supplementary information (ESI) available: ^{1}H-NMR and quantitative ^{13}C NMR spectra and LCST measurement of the poly(NIPAAm-*co*-AAm) copolymers; UV-vis absorption spectra of aqueous suspensions of Au nanocages before and after surface functionalization with poly(NIPAAm-*co*-AAm) copolymers; photograph showing the white spot on the bottom surface of the petri dish after irradiation with HIFU at a power of 15 W for 5 seconds; photographs of the chicken breast tissues with different thicknesses.

*Corresponding authors. xia@biomed.wustl.edu (for nanocage and polymer syntheses) and lhwang@biomed.wustl.edu (for high-intensity focused ultrasound experiments).
[b]Current address: Department of Biomedical Engineering, The State University of New York, Buffalo, NY 14260
[†]Weiyang Li, Xin Cai, and Chulhong Kim contributed equally to this work.

NIH-PA Author Manuscript
NIH-PA Author Manuscript
NIH-PA Author Manuscript

NIH-PA Author Manuscript

NIH-PA Author Manuscript

NIH-PA Author Manuscript

polymers for controlled release with NIR light through the photothermal effect.[3] However, the strong light scattering by biological tissue may limit the penetration depth, hindering the potential use of this light-based system in clinical applications.

High-intensity focused ultrasound (HIFU) has been a subject of interest for decades in medical research and is often considered to be attractive for cancer treatment because it is non-invasive or minimally invasive.[4] Unlike conventional radiation therapy, there is no maximum cumulative dose for focused ultrasound, so the treatment can be repeated until a tumor is destroyed.[5] Because of the significant acoustic energy deposition at the focus of HIFU, temperature rises rapidly, generating tissue necrosis at a minute spot with pinpoint accuracy. Additionally, a local temperature rise at the focus can be used for drug delivery to a specifically targeted region with minimum side effect on the surrounding tissue. Herein, we develop a platform for HIFU-induced, localized and controlled drug release that is based on Au nanocages covered with thermally-responsive polymers. In principle, this approach can also be extended to other hollow and porous particles made of materials other than Au, but Au offers major advantages such as easy surface modification via the gold-thiolate linkage. Moreover, because of the large optical absorption cross section and highly tunable LSPR properties of Au nanocages, we can further improve this system by combining optical imaging techniques with therapeutics for theranostic purposes.

Experimental

Chemicals and materials

N-isopropylacrylamide (NIPAAm, 99%) was obtained from Acros Organics (Thermo Fisher Science) and re-crystallized from hexane before use. Acrylamide (AAm, 99%) and 2,2′-azobis(isobutyronitrile) (AIBN, 95%) were both purchased from Aldrich and re-crystallized from methanol before use. Anhydrous diethyl ether 3,3′-dithiodipropionic acid, 1,4-dioxane, *N*,*N*′-dicyclohexylcarbodiimide (DCC), 4-(dimethylamino)pyridine (DMAP), and glutaric dialdehyde (50 wt%) were obtained from Aldrich and used as received without further purification. Rhodamine 6G (R6G, Acros Organics, Thermo Fisher Science) was used as received. Benzyl 2-hydroxyethyl carbonotrithioate was synthesized according to the literature.[6] Phosphate buffered saline (PBS) was purchased from Invitrogen, GIBCO. In all experiments, we used deionized water with a resistivity of 18 MΩ which was prepared using an ultrapure water system (MILLIPORE).

Synthesis of disulfide-containing chain transfer agent (CTA)

DCC (4.6 g, 22 mmol) and DMAP (0.25 g, 2 mmol) were added into a suspension of benzyl 2-hydroxyethyl carbonotrithioate (5.4 g, 22 mmol) and 3,3′-dithiodipropionic acid (2.1 g, 10 mmol) in 60 mL of anhydrous diethyl ether. The reaction mixture was stirred for 24 h and then filtered with celite. The filtrate was stored at 4 °C overnight and filtered with celite again. The crude product was further purified by silica gel flash column chromatography (15% ethyl acetate/hexane, v/v) to obtain the disulfide-containing CTA as yellow oil (1.6 g, 22% yield). ^{1}H NMR (300 MHz, CD_2Cl_2) δ 2.74 (t, J = 7.0 Hz, 4H), 2.92 (t, J = 7.0 Hz, 4H), 3.68 (t, J = 6.3 Hz, 4H), 4.33 (t, J = 6.3 Hz, 4H) 4.63 (s, 4H), 7.30-7.36 (m, 10H).

Synthesis of poly(NIPAAm-*co*-AAm) copolymers with LCST at 38.5 °C through RAFT polymerization

Disulfide-containing CTA (50 mg, 0.08 mmol) and 1,4-dioxane (40 mL) were added into a 100 mL argon-dried Schlenk flask and magnetically stirred for 5 min to obtain a homogeneous solution. NIPAAm (4.07 g, 36 mmol), AAm (0.284 g, 4 mmol), and AIBN (2.6 mg, 16 μmol) were added to this solution and stirred for 10 min. The reaction mixture was degassed through three cycles of freeze-pump-thaw. After the last cycle, the reaction

NIH-PA Author Manuscript

NIH-PA Author Manuscript

NIH-PA Author Manuscript

mixture was stirred for 10 min before being immersed in a pre-heated oil bath at 65 °C to start the polymerization. After 4.5 h, the NIPAAm monomer conversion reached ~75%, as measured by analyzing the collected aliquots with ^{1}H-NMR spectroscopy. The polymerization was quenched by cooling the reaction flask with liquid N_2. The copolymer was purified by precipitating it three times in 700 mL of diethyl ether at 0 °C. The precipitates were collected, washed with 200 mL of cold ether, and dried under vacuum overnight to obtain the copolymer as a yellow solid (3.0 g, 90% yield based on monomer conversion). ^{1}H NMR (600 MHz, CD_2Cl_2) δ 0.90 (br, N(C*H*$_3$)$_2$ Hs from the NIPAAm), 1.40 (br, copolymer backbone protons), 2.74 (t, C*H*$_2$ Hs from the CTA), 2.91 (t, C*H*$_2$ Hs from the CTA), 4.00 (br, C*H*N(CH$_3$)$_2$ Hs from the NIPAAm), 4.63 (br, 2Hs from the copolymer backbone methine terminus connected to trithiocarbonate), 6.50 (br, amide Hs from NIPAAm and AAm), 7.20 (br, Ar Hs); ^{13}C NMR (150 MHz, CD_2Cl_2) δ 23.0, 26.1, 30.6, 36.0, 41.8, 43.0, 67.6, 71.1, 125.8, 125.9, 128.8, 132.2, 136.5, 152.0, 164.8, 171.7, 174.7, 178.2.

Surface modification of Au nanocages with poly(NIPAAm-*co*-AAm) copolymers

The Au nanocages were synthesized using the galavanic replacement reaction between Ag nanocubes and chloroauric acid in water according to our published protocol.[7] A 5 mL aqueous suspension of Au nanocages (~8 pmol) was added dropwise, at a rate of 0.2 mL/min, into a 10 mL aqueous solution of poly(NIPAAm-*co*-AAm) copolymer (425 mg) in the absence of light. The mixture was stirred at 800 rpm for 5 days at room temperature. The solution was then centrifuged at 14,000 rpm for 15 min, and the supernatant was discarded. The copolymer-covered nanocages were then washed with water four times and re-suspended in 0.6 mL water.

Loading the copolymer-covered nanocages with dye

The aqueous suspension (0.6 mL) of copolymer-covered nanocages was mixed with 1.0 mL of R6G solution (5 mg/mL). The mixture was vortexed and sonicated for 5 min before being immersed in a pre-heated oil bath at 42 °C. After incubation at 42 °C overnight, the mixture was cooled in an ice bath for 1 h, and then centrifuged at 14,000 rpm and 20 °C for 15 min. The supernatant was discarded, and the R6G-loaded nanocages were washed with deionized water several times, until the absorbance of the supernatant at 527 nm measured using an ultraviolet-visible (UV-vis) spectrometer was less than 0.01.

Dye release from the copolymer-coated nanocages by conventional heating

Before dye release, the R6G-loaded Au nanocages were centrifuged and the supernatant was decanted. Warm water (40 °C, 0.6 mL) was added into the sample, which was immediately vortexed and incubated in a 40 °C oil bath for increasing periods of time. At intervals, the solution was cooled with an ice bath for 5 min, followed by centrifugation at 14,000 rpm and 20 °C for 15 min. The supernatant was then taken out for UV-vis spectral measurement, after which it was returned to the sample for further interval testing.

Dye release from the copolymer-coated nanocages by HIFU

Aqueous suspension (0.6 mL) of R6G-loaded nanocages was placed in a 1.5-mL centrifuge tube and then exposed to HIFU for different periods of time at a fixed power of 10 W. After exposure, the solution was cooled with an ice bath for 5 min, and centrifuged at 14,000 rpm and 20 °C for 15 min. The supernatant was taken out for UV-vis spectral measurement. A uniform gelatin film was cast to study the localized release of R6G by HIFU. The copolymers-covered Au nanocages (loaded with dye) were mixed with an aqueous gelatin solution (10 wt%) and added to a petri dish. Glutaric dialdehyde, a cross-linker, was then

NIH-PA Author Manuscript

NIH-PA Author Manuscript

NIH-PA Author Manuscript

added into the mixture. The petri dish was sealed with parafilm and put in the aqueous medium for HIFU treatment.

Instrumentation

The ^{1}H, ^{13}C, and quantitative ^{13}C NMR spectra of the as-prepared copolymers were recorded on a Varian 600 MHz spectrometer with CD_2Cl_2 as solvent and internal standard. Chemical shifts were referred to the proton resonance of the solvent. Gel permeation chromatography (GPC) with *N*,*N*-dimethylformamide (DMF) as a mobile phase was conducted on a chromatography system (Waters, Milford, MA) equipped with an isocratic pump model 1515, a differential refractometer, model 2414, and a two-column set of Styragel HR 4 and HR 4E 5 μm DMF 7.8 × 300 mm columns. The system was equilibrated at 70 °C in pre-filtered DMF containing 0.05 M LiBr, a polymer solvent and eluent (flow rate set to 1.00 mL/min). Polymer solutions were prepared at a concentration of ~ 3 mg/mL and injected at a volume of 200 μL. Data collection and analysis were performed with Empower Pro software (Waters). The system was calibrated with poly(ethylene glycol) standards (Polymer Laboratories) ranging from 615 to 442,800 Da. The lower critical solution temperature (LCST) of a polymer is defined as the temperature at which the light transmission of the polymer solution drops to 90% of the original value.[8] For the poly(NIPAAm-*co*-AAm) copolymer, we measured its LCST in both deionized water and PBS buffer solution (with a concentration of ~3 mg/mL) using a Varian Cary 100 Bio UV-vis spectrophotometer. The transmittance of the polymer solution at 600 nm was recorded over temperatures ranging from 25-70 °C, while the solution was heated at a rate of 1.0 °C/min.

Transmission electron microscopy (TEM) images were obtained with a Technai G2 Spirit microscope operated at 120 kV (FEI, Hillsboro, OR). Samples were prepared by dropping an aqueous suspension of particles on carbon-coated copper grids and drying at ambient temperature. The concentration of Au nanocages was determined using an inductively coupled plasma mass spectrometer (ICP-MS, Perkin Elmer): the concentration of Au ions was converted to the concentration of nanocages once the geometric dimensions of the nanocage had been determined from TEM images. Hydrodynamic diameters for the polymer-covered Au nanocages in aqueous solutions were determined using dynamic light scattering (DLS) with a Malvern Nano ZS DLS system (Malvern Instrument, Westborough, MA). UV-vis extinction spectra were recorded using a Cary 50 spectrometer (Varian, Palo Alto, CA). Fluorescent micrographs were taken using a QICAM Fast Cooled Mono 12-bit camera (Q Imaging, Burnaby, BC, Canada) attached to an Olympus microscope with Capture 2.90.1 (Olympus). All the images were taken with the same exposure parameters.

Results and discussion

Figure 1A shows a schematic of the experimental setup. The HIFU transducer (TX 009, Philips) was operated at a central frequency of approximately 1.6 MHz, with a focal length of 40 mm and a focal spot 0.9 mm in diameter. It was driven by a continuous sinusoidal voltage produced by a function generator (33250A, Agilent) and passed through a radiofrequency amplifier (240L, ENI). The HIFU transducer and the targeted sample were both immersed in a water bath to provide ultrasound coupling between them. Figure 1B illustrates how the controlled-release system works. The Au nanocages were typically synthesized using the galavanic replacement reaction between Ag nanocubes and chloroauric acid in water according to the published protocol.[7] The surface of the nanocages was functionalized with thermally-responsive copolymers, poly(NIPAAm-*co*-AAm) (NIPAAm: N-isopropylacrylamide; AAm: acrylamide), by means of the gold-thiolate linkage. These copolymers can change conformation in response to temperature variations at a transition point known as the LCST.[8] When the temperature of the solution is below its

NIH-PA Author Manuscript

NIH-PA Author Manuscript

NIH-PA Author Manuscript

LCST, the polymer is hydrophilic and solvated by water. As the temperature increases beyond its LCST, the polymer undergoes a phase transition and becomes collapsed and highly hydrophobic. This conformational change with temperature is reversible, allowing one to control the dosage of drug release by altering the duration in which the polymer chains are kept at the high-temperature state. When a significant amount of acoustic energy is delivered to the focus using HIFU, the temperature in the focal volume of the sample increases rapidly. As the temperature rises beyond the LCST of the copolymer, the polymer chains change from a stretched conformation to a collapsed state. As a result, the pores on the nanocages are opened, releasing the chemical or drug pre-loaded in the nanocages. When HIFU is turned off, the temperature drops to its original state and the polymer chains relax back to their extended conformation, blocking the pores and thus terminating the release. The released dosage can be remotely controlled by manipulating the power and/or the duration of HIFU irradiation. It should be pointed out that the temperature-sensitive polymers – for example, poly(NIPAAm) and its derivatives -- have also been used for a number of other drug delivery systems including poly(NIPAAm)-capped particles of mesoporous silica and cross-linked hollow capsules of poly(NIPAAm).[9]

The smart copolymers, poly(NIPAAm-*co*-AAm), used in the present work were prepared by reversible addition-fragmentation chain transfer (RAFT) radical polymerization instead of the atom-transfer radical polymerization (ATRP) method used in our previous study.[3] RAFT radical polymerization offers a number of advantages over ATRP: *i*) it can eliminate the tedious purification step that often involves dialysis over a long period of time; *ii*) it is free of residual Cu species (associated with the catalyst for ATRP), which could complicate their applications in biomedical research; and *iii*) copolymers prepared with RAFT show a much narrower molecular weight distribution, with a polydispersity index (PDI) of 1.3, compared to those synthesized using ATRP (PDI >1.6). As schematically shown in Figure 1C, RAFT copolymerization of NIPAAm and AAm monomers (at a molar feeding ratio of 9 to 1) was carried out in 1,4-dioxane at 65 °C in the presence of a disulfide-containing chain transfer agent (CTA) and 2,2′-azobis(isobutyronitrile) (AIBN, a thermal initiator). The ^{1}H-NMR spectra of the purified copolymers shown in Figure S1 (see Supporting Information) clearly indicates the existence of CTA (resonances at 2.74, 2.91, and 7.10-7.30 ppm) across the copolymer backbone, with corresponding integral ratios of 1:1:2.2, further confirming a well-defined structure for the poly(NIPAAm-*co*-AAm) copolymers. The composition of the copolymer was determined using quantitative ^{13}C-NMR spectroscopy (Fig. S1) through a comparison of the integral values of two types of amide carbonyls: primary amide for the AAm residue at 178.2 ppm and secondary amide for the NIPAAm residue at 174.7 ppm. From the quantitative ^{13}C NMR analysis, the molar ratio between the two different repeating units was determined to be $N_{\mathrm{NIPAAm}}/N_{\mathrm{AAm}} \approx 9{:}1$, which was very close to the feeding ratio of the monomers. Furthermore, our thermo-responsive measurements showed that the LCST of the copolymer in deionized water and PBS buffer solution was 38.5 and 37.7 °C (Fig. S2), respectively, which are between the human physiological temperature (37 °C) and hyperthermia (42 °C).

Figure 2A shows typical TEM images of the Au nanocages after being functionalized with poly(NIPAAm-*co*-AAm). The nanocages were about 52 nm in edge length, with a wall thickness of around 9 nm. The pores on the surface of the nanocages were, on average, 7 nm in size, and the thickness of the copolymer on the cage surface was around 3 nm in the dry state (inset of Fig. 2A). The hydrodynamic diameter (measured by dynamic light scattering) of the nanocages increased from 110 to 137 nm after surface functionalization with the copolymer. Also, the LSPR peak of the nanocages shifted from 754 to 780 nm (Fig. S3). Both results indicate that the copolymers were successfully grafted to the surface of the nanocages. Figure 2B shows a TEM image of the Au nanocages after irradiation with HIFU

NIH-PA Author Manuscript

NIH-PA Author Manuscript

NIH-PA Author Manuscript

at 12 W for 20 min. Although a relatively high power was used, no structural change to the nanocages was observed (inset of Figure 2B).

We used rhodamine 6G (R6G) as a fluorescent dye to demonstrate the capability of controlled release. This dye is similar to doxorubicin, a commonly used drug for cancer chemotherapy, in terms of molecular weight (similar size) and surface charges.[10] Since R6G has a strong absorption peak at 527 nm, its release could be easily monitored by UV-vis spectra of the supernatants at different time points after the nanocages had been centrifuged down. To load the dye, the copolymer-covered nanocages were added to an aqueous solution of R6G and stirred at 42 °C overnight. Then, the suspension was quickly cooled with an ice bath to trigger a conformational change for the copolymer, blocking the pores and keeping the loaded dye inside the nanocages.

Figure 3, A and B, compares the release of R6G when the dye-loaded nanocages were heated at 40 °C and irradiated by HIFU at a power of 10 W, respectively, for different periods of time. It can be seen that the intensity of optical absorption peak for R6G increased with the duration of heating or HIFU irradiation, indicating that the released dosage could be controlled by varying the amount of heat delivered to the system. As heating was prolonged, the total amount of R6G released into the solution kept increasing, but eventually leveled off. By referring to a calibration curve separately prepared for the same dye, we determined the exact concentration of R6G released from the nanocages at different time points, as shown in Figure 3C. The release profiles indicate that more dye was released within the same period of time when the release was triggered by HIFU than by conventional heating, and the release rate was also higher for the system with HIFU. The concentration of the released R6G was about 2.15 μM when exposed to HIFU for 5 min, while it took more than 20 min for the same concentration of R6G to be released by conventional heating. In addition, when HIFU was used to trigger the release, most of the dye was released in 10 min, and the concentration of the released dye increased only about 0.1 μM from 10 to 20 min, and then essentially did not change after 20 min. A control experiment of release at the human physiological temperature (37 °C) was also conducted, and no obvious release was observed (less than 0.06 μM) after the dye-loaded nanocages had been heated at 37 °C for 48 h (Fig. S4).

The fast response associated with HIFU can be attributed to the rapid local temperature rise within the focal volume achieved by the focused-ultrasound wave. Figure 4 shows the temperature increase measured at the focal volume of HIFU (about 4.26 μL, the focal volume was considered as a cylinder with a diameter of 0.9 mm and a height of 6.7 mm) for aqueous suspensions of Au nanocages (0.1 nM) after exposure to HIFU for different periods of time and at different powers. The temperature could increase from about 35 °C to 41.2, 39.6, 37.6 °C in 1 min, and saturated at 43, 41 and 39 °C after 2 min, at powers of 10 W , 8 W , and 6 W, respectively. In addition, the rate of temperature rise increased with the power. Because more heat was generated by HIFU than conventional heating, the copolymer could maintain its conformation in an extended state for a longer period of time, keeping the pores on the nanocages open for a longer period of time to release more dye molecules.

The rapid temperature rise within the focal volume induced by HIFU can be used to trigger a highly localized release. We investigated this feasibility by using gelatin phantoms made from a mixture of gelatin solution and Au nanocages pre-loaded with the dye. As described in the experimental section, the mixture was added into a petri dish to cast into a uniform, dark-blue gelatin film (inset of Figure 5A). The dark-blue color can be attributed to the presence of Au nanocages. In a typical procedure, we first focused the HIFU on the bottom surface of the petri dish at a relatively high power (15 W) for 5 second to generate a tiny white spot (Figure S5), which would allow us to easily locate the release spot under a

NIH-PA Author Manuscript

NIH-PA Author Manuscript

NIH-PA Author Manuscript

fluorescence microscope. We then reduced the power to a lower level (e.g., 10 W or a less) and moved the focal point vertically into the gelatin phantom. Figure 5A shows fluorescence microscopy image taken from the gelatin phantom with dye-loaded nanocages before HIFU irradiation and it served as a control. The dye molecules encapsulated in the Au nanocages were not expected to fluoresce due to the quenching effect of the Au surface.[11] Figure 5, B and C, show two typical fluorescence microscopy images of the gelatin phantoms after exposed to HIFU at a power of 10 W for 2 and 20 min, respectively. It can be observed that only a small area around the focal volume exposed to HIFU showed release of the dye. The fluorescence intensity of the released dye was obviously increased from 2 to 20 min. The release pattern was more or less circlar in each image, suggesting the involvement of dye diffusion and heat dissipation from the focal point. The contrast difference in the center of each image (the relatively dark area) was caused by the mark we generated on the bottom surface of the petri dish. We also took fluorescence microscopy images of the gelatin phantoms after exposed to HIFU at powers of 6 and 8 W, respectively, for 2, 5, 10, and 20 min. The images were similar to those in Figure 5, B and C, except the difference in fluorescence intensity. Figure 5D shows the normalized fluorescence intensity as a function of time, where the data were calculated from the fluorescence images. The average value from the image shown in Figure 5A was considered as the background. The corresponding fluorescence intensity of each image was obtained by eliminating the background and averaging the values of the remaining pixels. Each data point was then normalized against the average fluorescence intensity for the image of a gelatin phantom taken after exposed to HIFU at a power of 6 W for 2 min. It can be observed that the fluorescence intensity increased with the duration of time exposed to HIFU for the same power, which is consistent with the results obtained from the UV-vis measurements (shown in Figure 3B). At the same duration of HIFU exposure, the fluorescence intensity increased with increasing power.

We also evaluated the capability to release at a deep penetration depth with HIFU by adding chicken breast tissue to the top of the gelatin phantom. Figure 6A shows fluorescence microscopy image of the sample (containing dye-loaded Au nanocages) covered with a chicken breast tissue of 15 mm thick, after HIFU irradiation at a power of 10 W for 20 min. The fluorescence intensity was reduced relative to the sample under the same experimental conditions without chicken tissue (Figure 5C), indicating stronger attenuation of ultrasound by soft tissue than by water. However, the release of dye was still visible as indicated the strong fluorescence signal shown in Figure 6A, indicating the excellent penetration ability of HIFU. The diamater of the released region was about 6 mm. When a second layer of chicken breast tissue was added (with a total thickness of 30 mm), release of the dye could still be observed, even though the fluorescence intensity was further reduced (Figure 6B). We did not add more layers of chicken breast tissue because the HIFU transducer we used was limited to a focal length of 40 mm. However, we believe that deeper penetration depths can be achieved by modifying the focal length of the tranducer as well as by manipulating the power and irradiation time.

Conclusions

In summary, we have successfully demonstrated a new platform based on Au nanocages covered with thermally-responsive polymers for HIFU-induced drug release. HIFU can rapidly induce a local temperature rise in the focal volume, and thus greatly increase release rate over the system triggered with conventional heating. Localized release was also demonstrated by taking fluorescence microscopy images from gelatin phantoms containing the dye-loaded Au nanocages after HIFU exposure at different powers for different periods of time. Only a small region around the focal volume of HIFU showed release of the dye. The fluorescence intensity of the released dye increased with increasing power at a fixed exposure time. In addition, by placing chicken breast tissue on top of the gelatin phantom, a

NIH-PA Author Manuscript

NIH-PA Author Manuscript

NIH-PA Author Manuscript

penetration depth of at least 30 mm was demonstrated. We believe that the combination of smart polymer-covered nanocages and HIFU holds great promise in controlled release for various biomedical applications.

Supplementary Material

Refer to Web version on PubMed Central for supplementary material.

Acknowledgments

This work was supported in part by a 2006 NIH Director's Pioneer Award (DP1 OD000798) and startup funds from Washington University in St. Louis (to X.Y.). This work was also sponsored by NIH grants (No. R01 EB000712, No. R01 EB008085, No. R01 CA134539, and No. U54 CA136398, to L.V.W). Part of the research was performed at the Nano Research Facility (NRF), a member of the National Nanotechnology Infrastructure Network (NNIN), which is supported by the NSF under ECS-0335765. L.V.W. has a financial interest in Microphotoacoustics, Inc. and Endra, Inc., which, however, did not support this work.

References

1. See, for example, a) Sperling RA, Gil PR, Zhang F, Zanella M, Parak WJ. Chem. Soc. Rev. 2008; 37:1896. [PubMed: 18762838] b) Ghosh P, Han G, De M, Kim CK, Rotello VM. Adv. Drug Del. Rev. 2008; 60:1307. c) Wilson, Robert. Chem. Soc. Rev. 2008; 37:2028. [PubMed: 18762845] d) Boisselier E, Astruc D. Chem. Soc. Rev. 2009; 38:1759. [PubMed: 19587967] e) Cho EC, Kim C, Zhou F, Cobley CM, Song KH, Chen J, Li Z, Wang LV, Xia Y. J. Phys. Chem. C. 2009; 113:9023.
2. a) Chen J, Saeki F, Wiley BJ, Cang H, Cobb MJ, Li Z-Y, Au L, Zhang H, Kimmey MB, Li X, Xia Y. Nano Lett. 2005; 5:473. [PubMed: 15755097] b) Chen J, Wang D, Xi J, Au L, Siekkinen A, Warsen A, Li Z-Y, Zhang H, Xia Y, Li X. Nano Lett. 2007; 7:1318. [PubMed: 17430005] c) Chen J, Glaus C, Laforest R, Zhang Q, Yang M, Gidding M, Welch MJ, Xia Y. Small. 2010; 6:811. [PubMed: 20225187] d) Song KH, Kim C, Cobley CM, Xia Y, Wang LV. Nano Lett. 2009; 9:183. [PubMed: 19072058] e) Kim C, Cho EC, Chen J, Song KH, Au L, Favazza C, Zhang Q, Cobley CM, Gao F, Xia Y, Wang LV. ACSNano. 2010; 4:4559. f) Chen J, Yang M, Zhang Q, Cho EC, Cobley CM, Kim C, Glaus C, Wang LV, Welch MJ, Xia Y. Adv. Func. Mater. 2010; 20:3684.
3. Yavuz MS, Cheng Y, Chen J, Cobley CM, Zhang Q, Rycenga M, Xie J, Kim C, Song KH, Schwartz AG, Wang LV, Xia Y. Nature Mater. 2009; 12:935. [PubMed: 19881498]
4. a) Kennedy JE, ter Haar GR, Cranston D. Br. J. Radiol. 2003; 76:590. [PubMed: 14500272] b) Haar GT, Coussios C. Int J. Hyperthermia. 2007; 23:85. [PubMed: 17578334]
5. Haar GT, Coussios C. Int J. Hyperthermia. 2007; 23:89. [PubMed: 17578335]
6. Hales M, Barner-Kowollik C, Davis TP, Stenzel M. H. Langmuir. 2004; 20:10809.
7. Chen J, McLellan JM, Siekkinen A, Xiong Y, Li Z, Xia Y. J. Am. Chem. Soc. 2006; 128:14776. [PubMed: 17105266]
8. Hoffman AS. Adv. Drug Deliv. Rev. 2002; 43:3. [PubMed: 11755703]
9. a) Hoffman AS. Adv. Drug Deliv. Rev. 2002; 43:3. [PubMed: 11755703] b) Zhao Y, Vivero-Escoto JL, Slowing II, Trewyn BG, Lin VS-Y. Expert Opin. Drug Deliv. 2010; 7:1013. [PubMed: 20716017] c) Zhang JT, Huang SW, Cheng SX, Zhuo RX. J. Polym. Sci. Part A: Polym. Chem. 2004; 42:1249. d) Nayak S, Lee H, Chmielewski J, Lyon LA. J. Am. Chem. Soc. 2004; 126:10258. [PubMed: 15315434] e) Ichikawa H, Fukumori Y. J. Cont. Release. 2000; 63:107. f) Slowing II, Vivero-Escoto JL, Trewyn BG, Lin VS-Y. J. Mater. Chem. 2010; 20:7924.
10. Wu EC, Park JH, Park J, Segal E, Cunin F, Sailor MJ. ACS Nano. 2008; 2:2401. [PubMed: 19206408]
11. a) Mayilo S, Kloster MA, Wunderlich M, Lutich A, Klar TA, Nichtl A, Kürzinger K, Stefani FD, Feldmann J. Nano Lett. 2009; 9:4558. [PubMed: 19921780] b) Dulkeith E, Morteani AC, Niedereichholz T, Klar TA, Feldmann J. Phys. Rev. Lett. 2002; 89:203002–1. [PubMed: 12443474]

NIH-PA Author Manuscript

NIH-PA Author Manuscript

NIH-PA Author Manuscript

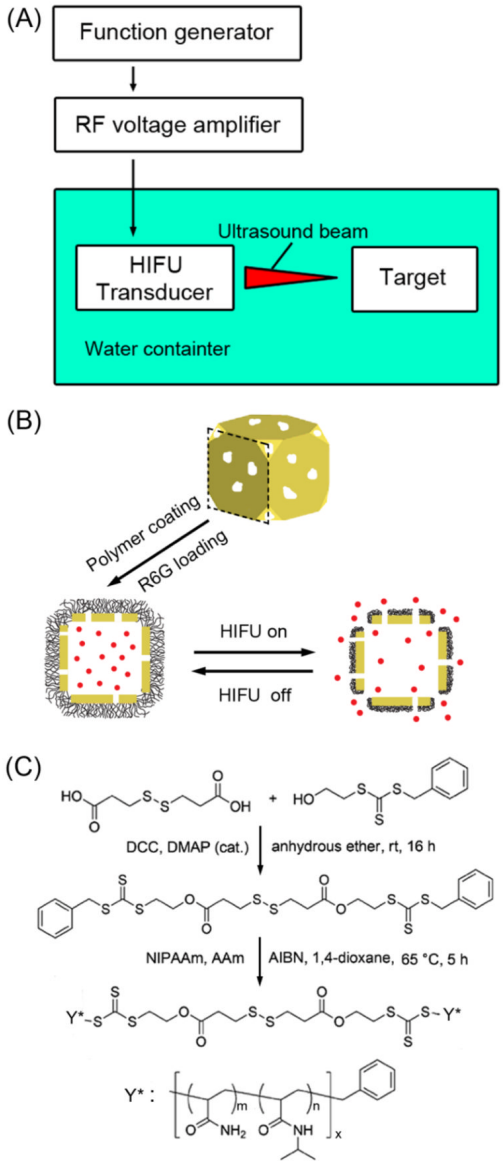

Figure 1.

Schematic illustrations showing (A) setup for the high-intensity focused ultrasound (HIFU) experiments, (B) how the controlled-release system works; and (C) procedure for the synthesis of poly(NIPAAm-*co*-AAm) copolymers through RAFT copolymerization. DCC: *N*,*N*′-Dicyclohexylcarbodiimide; DMAP: 4-Dimethylaminopyridine.

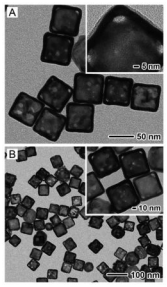

Figure 2.
TEM images of (A) the Au nanocages functionalized with poly(NIPAAm-*co*-AAm) and (B) the same sample after the dye had been released by triggering with HIFU. The inset of (A) shows a magnified TEM image of the corner region of such a nanocage. The inset of (B) shows an enlarged TEM image of the nanocages after exposure to HIFU, indicating that no structural change occurred during the exposure.

NIH-PA Author Manuscript NIH-PA Author Manuscript NIH-PA Author Manuscript

NIH-PA Author Manuscript

NIH-PA Author Manuscript

NIH-PA Author Manuscript

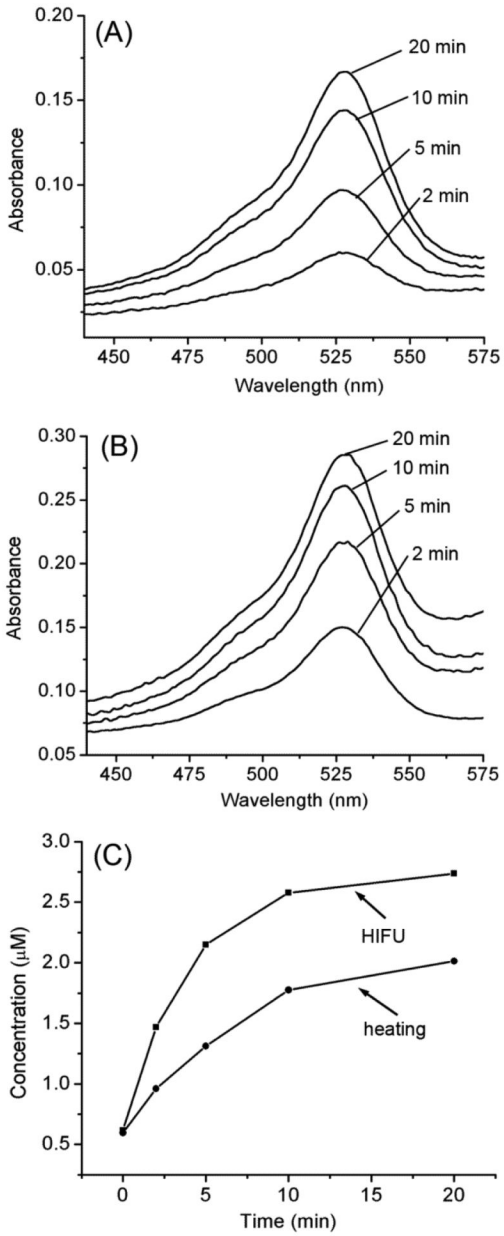

Figure 3.

Controlled release of R6G from Au nanocages covered by a copolymer with an LCST at 38.5 °C. The absorption spectra were taken after the samples had been (A) heated at 40 °C for 2, 5, 10, and 20 min and (B) exposed to HIFU at a power of 10 W for 2, 5, 10, and 20 min. (C) A comparison of the concentration profiles of R6G released from the nanocages triggered by conventional heating and HIFU, respectively.

NIH-PA Author Manuscript

NIH-PA Author Manuscript

NIH-PA Author Manuscript

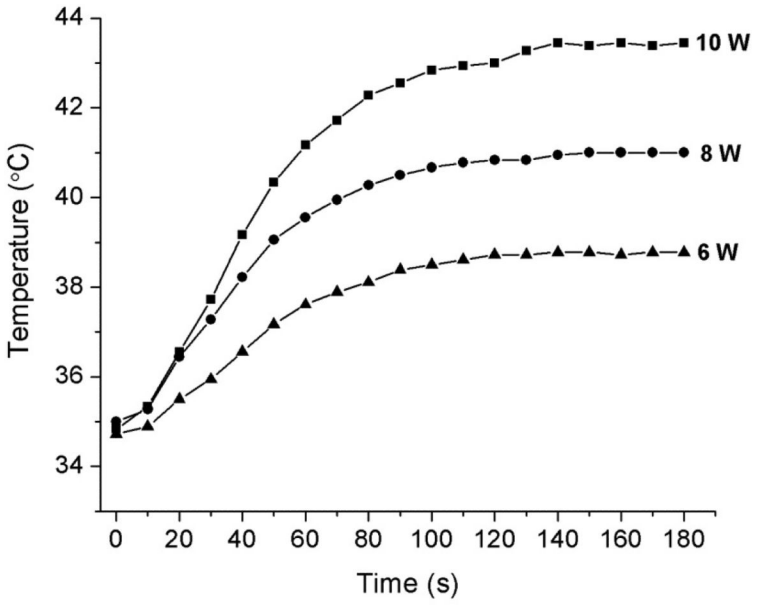

Figure 4.
The changes in temperature measured at the focal volume of HIFU for aqueous suspensions of Au nanocages (0.1 nM) after exposed to HIFU at different powers for different periods of time.

NIH-PA Author Manuscript
NIH-PA Author Manuscript
NIH-PA Author Manuscript

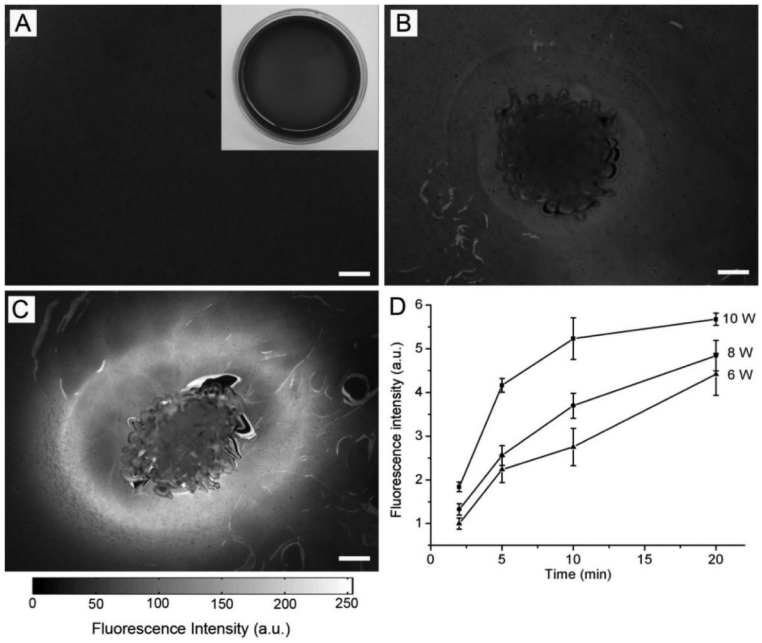

Figure 5.

Fluorescence microscopy images of the gelatin phantom with dye-loaded Au nanocages (A) before and (B, C) after exposure to HIFU at a power of 10 W for 2 and 20 min, respectively. The scale bar corresponds to 500 μm, and applies to all images. The inset of (A) shows a photograph of the gelatin phantom in a petri dish prepared from a mixture of gelatin solution and Au nanocages pre-loaded with the dye. (D) The normalized fluorescence intensity as a function of time calculated from fluorescence microscopy images of the gelatin phantoms after exposure to HIFU for different periods of time (2, 5, 10, and 20 min) and at different powers (6, 8, and 10 W). Each data point represents three measurements and was obtained by normalizing against the average fluorescence intensity of the sample exposured to HIFU at a power of 6 W for 2 min.

NIH-PA Author Manuscript

NIH-PA Author Manuscript

NIH-PA Author Manuscript

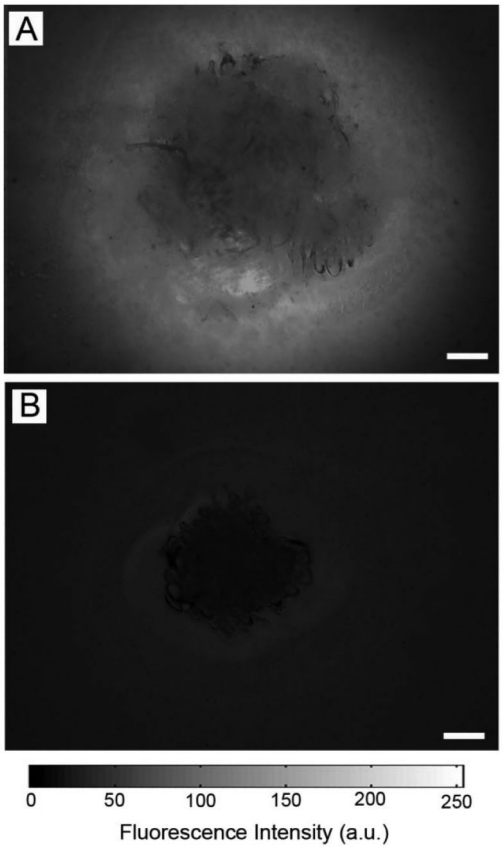

Figure 6.
Fluorescence microscopy images of the gelatin phantoms that were covered with chicken breast tissues of two different thicknesses and then exposed to HIFU: (A) 15 mm and (B) 30 mm. The scale bars correspond to 500 μm.